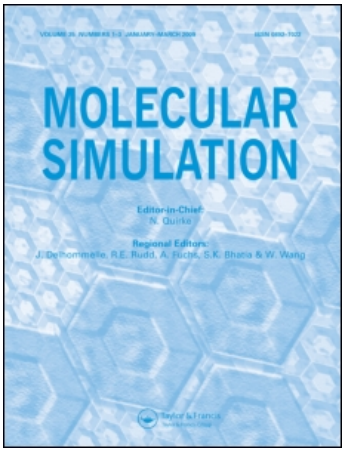


**Molecular Simulation**
Publication details, including instructions for authors and subscription information:
http://www.informaworld.com/smpp/title~content=t713644482

# Interaction of liquid water with the rutile $TiO_2$ (110) surface

A. A. Skelton[a]; T. R. Walsh[a]
[a] Department of Chemistry and Scientific Computing, University of Warwick, Coventry, UK

**To cite this Article** Skelton, A. A. and Walsh, T. R.(2007) 'Interaction of liquid water with the rutile $TiO_2$ (110) surface', Molecular Simulation, 33: 4, 379 — 389
**To link to this Article: DOI:** 10.1080/17441690701191693
**URL:** http://dx.doi.org/10.1080/17441690701191693

*Molecular Simulation*, Vol. 33, Nos. 4–5, 15–30 April 2007, 379–389

Taylor & Francis
Taylor & Francis Group

# Interaction of liquid water with the rutile $TiO_2$ (110) surface

A. A. SKELTON* and T. R. WALSH

Department of Chemistry and Scientific Computing, University of Warwick, Coventry CV4 7AL, UK

*(Received June 2006; in final form December 2006)*

A force-field which describes the interaction between the $TiO_2$ (110) rutile surface and a modified TIP3P water [P. Mark and L. Nilsson, *J. Phys. Chem. A*, **105**, 9954, (2001)] is tested against periodic density functional theory (PDFT). Optimizations of water on the non-hydroxylated and hydroxylated surfaces are performed using PDFT and the geometries are compared with optimizations of modified TIP3P water on the $TiO_2$ surface using the force-field. The surface hydroxyl torsional profile is also compared using PDFT and force-field calculations as well as molecular dynamics (MD) simulations of the surface. MD simulations of liquid TIP3P water, containing dissolved $Na^+$ and $Cl^-$ ions, on six $TiO_2$ (110) surfaces at 298 K and 1 atm are performed for neutral surfaces and negatively-charged surfaces. Axial density and angular distributions show good agreement with results of Predota *et al.* [*J. Phys. Chem. B*, **108**, 12049 (2004)] and X-ray crystal truncation rod experiments [Z. Zhang *et al.*, *Langmuir*, **20**, 4954 (2004)].

*Keywords*: Liquid water; Rutile surface; Periodic density functional theory; Molecular dynamics simulations



## 1. Introduction

Mineral–aqueous interfaces are of great importance in many aspects of technology and natural systems [1]. Titanium dioxide ($TiO_2$) is commonly used as a model system to study these interfaces but it also has applications in biotechnology. Proteins adsorbed on $TiO_2$ can be used as biosensors [2–4] or in the controlled placement and assembly of materials [5] in electronic devices due to the electronic conduction properties of titania.

Experimental controversy remains regarding the dissociation state of $TiO_2$ under bulk water [6,7]. There is a great deal of data on $TiO_2$ under ultra high vacuum conditions (scanning tunnelling microscopy, STM) [8] and temperature programmed desorption (TPD) [9] experiments) but obtaining data for $TiO_2$ under bulk water is more challenging.

Many *ab initio* studies have been performed to address this problem [10–16]. Zhang and Lindan [15] examined dissociation of water on the surface using density functional theory (DFT) and concluded that there are mixed dissociation states. A more recent study used DFT to look at the energetics of rutile $TiO_2$ (110) under different acidic and basic conditions by looking at surfaces with a differing coverage of associative and dissociative water [16].

The first force-field developed for $TiO_2$ was that of Matsui and Akoagi [17]. It was used only for bulk $TiO_2$ and the parameters were determined to reproduce observed crystal structures of rutile, anatase and brookite. Bandura *et al.* [18,19] performed PDFT and cluster calculations and derived force-field parameters from them [20] which could then describe the surface. Simulations describing the interface between the $TiO_2$ (110) surface and SPC/E water were performed using this force-field [21]. Simulations of dipeptides on the bare $TiO_2$ surface under aqueous conditions have been recently reported [22]. The authors used TIP3P water in conjunction with the AMBER force-field [23,24].

The emphasis for this study is that it is a precursor for further studies of the interaction between rutile $TiO_2$ and biological molecules, specifically peptides and proteins. Since water is always present in such systems it is vital that we adequately describe the interaction between $TiO_2$ and water. In our future studies, we aim to use modified TIP3P water [25,26]. The reason for this is that the modified TIP3P water model [26] was developed with and extensively tested against the CHARRM27 force-field [27] which we intend to use for simulations with peptides and water. We therefore want to compare the modified TIP3P model with the SPC/E model, which is the existing water model used for aqueous/$TiO_2$ interfaces. It would

*Corresponding author. Email: a.a.skeleton@warwick.ac.uk

*Molecular Simulation*
ISSN 0892-7022 print/ISSN 1029-0435 online © 2007 Taylor & Francis
http://www.tandf.co.uk/journals
DOI: 10.1080/17441690701191693

not be possible to use a model, which incorporates the dissociation of water because of the complexity and therefore expense of such calculations at the large scale used in this study. For this reason, a range of dissociation states were considered and it is hoped that by putting the information of all dissociation states together a picture of the real system can be found. Some of these surfaces are charged and this could prove useful because charged sites have been identified as possible key sites for binding of charged groups of biomolecules [28].

## 2. Methods

### 2.1 Force field

The water model used throughout this work was the modified TIP3P [26] (table 1). The charges for the non-hydroxylated $TiO_2$ surface were taken from Predota *et al.* [21]. A different charge set was used for neutral and negative surfaces so that removing a bridging hydrogen or adding a terminal hydroxyl would result in a $-1$ charge on the surface. These were also taken from Predota *et al.* [21]. The Lennard–Jones parameters for the surface hydrogens and oxygens were taken from the TIP3P hydrogen and oxygen, respectively. Lorentz–Berthelodt rules were used in order to calculate van der Waals (VDW) interactions. The TIP3P water parameters were taken from the TINKER package [26,29] and have VDW parameters for the hydrogens, which we recognise is not the standard TIP3P force-field. A harmonic potential was used to describe bonding between oxygens and hydrogens for the bridging and terminal hydroxyls and the parameters are given in table 2.

### 2.2 Validation of force field

In order to test the force field, periodic density functional theory (PDFT) calculations were performed. All calculations used the CASTEP package [30] with four *k*-points with a 400 eV cutoff energy using ultrasoft psuedopotentials [31]. We used the revised Perdew–Burke–Ernzerhof (RPBE) functional [32]. For the optimization of the water on the hydroxylated surface using PDFT, a five layer $TiO_2$ slab was used with cell dimensions of $6.499 \times 6.1874 \times 30.0$ Å. This corresponds to a $1 \times 2$ unit cell with a vacuum gap in the *z*-direction of about 20 Å. The slab was generated by cleaving the experimental bulk structure and optimizing using the PDFT with the above conditions.

Table 1. Atomic charges and Lennard–Jones parameters for water and hydroxyl atoms where $E_{ij} = \sqrt{\varepsilon_i \varepsilon_i}[(r_m + r_m/(2r_i))^{12} - 2(r_m + r_m/2r_i)^6] + q_i q_j/4\pi\varepsilon_0 r_{ij}$.

| *Atom* | *q (e)* | $r_m$ (Å) | $\varepsilon_i$ (kcal mol$^{-1}$) |
|---|---|---|---|
| H | 0.417 | 0.2245 | 0.0460 |
| O | −0.834 | 1.7682 | 0.1521 |
| Ti (five-coordinated)–O (water) pair | – | 3.7 | 0.032 |

Table 2. Bonding potential parameters where $E_{\text{Bonding}} = \sum k_b(b - b_0)^2$.

| *Bonding pair* | $b_0$ (Å) | $k_b$ (kcal mol$^{-1}$) |
|---|---|---|
| O—H (terminal) | 0.9708 | 400.00 |
| O—H (bridging) | 0.9766 | 400.00 |
| O—H (water) | 0.9572 | 450.00 |

PDFT single point energy calculations were made at regular intervals of the dihedral angle corresponding to rotation of one of the terminal hydrogens on the hydroxylated surface. In this way, the change in potential energy as the hydrogen was rotated was calculated. A three layer $TiO_2$ structure was used with cell dimensions of $6.499 \times 6.1874 \times 30.0$ Å. This process was repeated using the force-field.

### 2.3 Car–Parinello molecular dynamics (CPMD)

A CPMD simulation was performed for 8 ps with a time step of 0.01 ps using the CASTEP package [29]. The canonical (*NVT*) ensemble was used at a temperature of 300 K. one *k*-point was used with a cutoff of 400 eV, ultrasoft psuedopotentials [31] and using the RPBE functional. A cell dimension of $6.499 \times 6.1874 \times 30.0$ Å was used and all atoms were kept fixed except for bridging and terminal hydroxyls. No water molecules were present in these simulations.

### 2.4 Simulation details

The molecular dynamics (MD) simulations were performed using the TINKER package [29]. For all simulations, a five-layer slab was used. No vacuum layer was used in between one surface layer and the other because it has been shown to be unimportant for atom density profiles [33]. The non-hydroxylated surface (figure 1(b)) was a replica of the experimental unit cell [34,35]. The negative non-hydroxylated surfaces were then made by addition of the desired number of hydroxyls. Here we followed the structural model of Predota *et al.* [21]. The hydroxylated surface (figure 1(a)) was derived by placing hydroxyls on all five-coordinated Ti sites and placing protons on all bridging oxygen sites and fully optimizing using PDFT under the conditions mentioned previously. Negatively-charged hydroxylated surfaces were then made by removing 25 and 12.5% of the bridging hydroxyl protons and again, the structural models of Predota *et al.* were followed. The non-hydroxylated bridging oxygens in this case were fixed. Negative non-hydroxylated surfaces were made by putting hydroxyls on 25 and 12.5% of the five-coordinated titanium sites as in Predota *et al.* [21]. In order to balance the extra negative charge in the cell, $Na^+$ ions were added to the water.

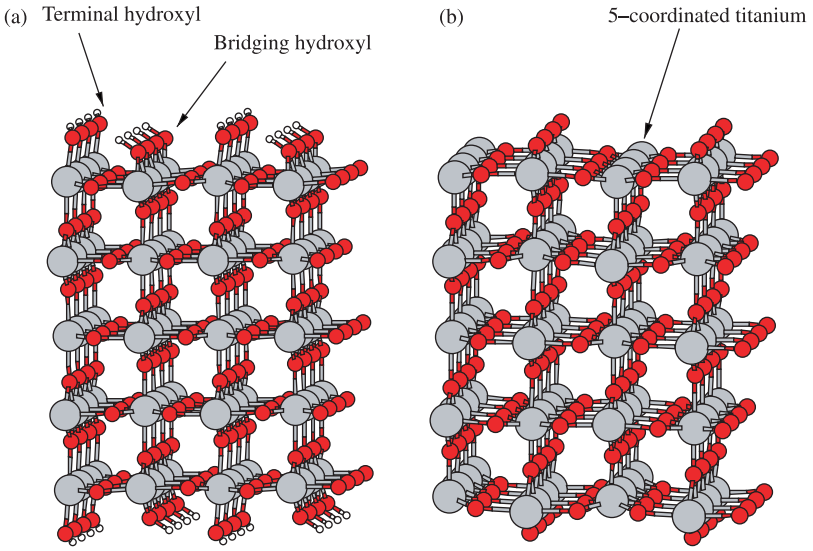


Figure 1. Structure of hydroxylated (a) and non-hydroxylated surface (b) of rutile $TiO_2$ (110) surface.



18 $Na^+$ ions and two $Cl^-$ ions were added to the 25% surfaces and 10 $Na^+$ ions and two $Cl^-$ ions to the 12.5% surfaces. All simulations were done using the isobaric–isothermal (*NPT*) ensemble at 1 atm pressure and a temperature of 298 K. The simulations were run for 1 ns with a time step of 1 fs and the frames being saved every 500 fs. The Verlet algorithm [36] and 12 Å cutoff were used for all simulations. The initial cell dimension was 25.996 × 24.7496 × 75 Å with $z$-typically compressing to about 55 Å. About 870 water molecules were simulated.

## 3. Results

### *3.1 PDFT calculations of torsion energy profile for surface hydroxyls*

PDFT single point energy calculations were made at regular intervals of the dihedral angle corresponding to rotation of one of the terminal hydrogens. In this way, the change in potential energy as the hydrogen was rotated was calculated. The same torsional profile was calculated using the force-field and the comparison is shown in figure 2. It can be seen that the energy profile follows a similar shape with the highest energy occurring when the hydrogens are closest to each other.

An optimization of the surface was made using an angle bending potential like that used in Bandura and Kubicki [20]. That is a $k = 14.136\,\text{kcal mol}^{-1}\,\text{rad}^{-2}$ where $E_b = (1/2)k(\theta - \theta_0)^2$ for both the Ti–O–H angles. The bridging hydrogens moved so that they were unphysically close to the bridging titanium atoms upon optimization. This should not happen because in reality there would be repulsion between the bridging hydrogen and titanium atoms. In order to overcome this problem without fixing the angle, the 1–3 electrostatic interaction between the surface titanium atoms and the hydroxyl hydrogen was included.

These optimizations also gave information about the bending potential between the terminal hydrogen, oxygen and titanium. In the optimizations, it was obvious that our original bending constant was not large enough because the angle would decrease after optimization. For this reason, it was increased from $14.136\,\text{kcal mol}^{-1}\,\text{rad}^{-2}$ to $100.0\,\text{mol}^{-1}\,\text{rad}^{-2}$. The bridging hydroxyl Ti–O–H bending constant was also changed to $100.0\,\text{mol}^{-1}\,\text{rad}^{-2}$ (table 3).

### *3.2 CPMD calculations*

It is assumed in the energy profile calculations that when the terminal hydrogen is rotated and approaches another one that this hydrogen will itself rotate in order to move

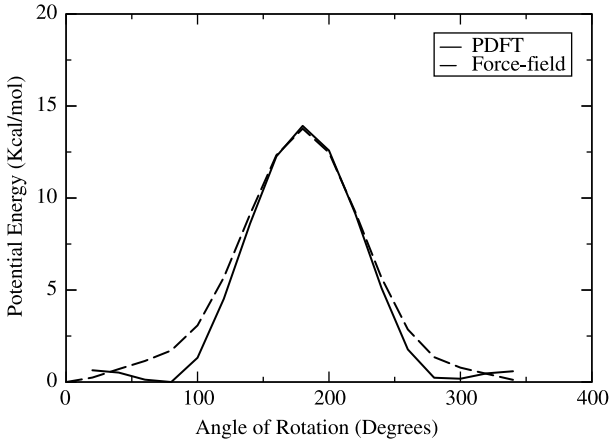


Figure 2. Torsional energy profile of terminal hydroxyl using the force-field and PDFT for the fully hydroxylated surface.

Table 3. Parameters of the H–O–H and Ti–O–H angle bending where $E = (1/2)k(\theta - \theta_0)^2$.

| *Bending mode* | $\theta_0$ *(deg)* | *kcal mol*$^{-1}$ *rad*$^{-2}$ |
|---|---|---|
| H—O—H | 104.52 | 55.00 |
| Ti—O—H terminal | 115.375 | 100.00 |
| Ti—O—H bridging | 111.557 | 100.00 |

away. For this reason, CPMD calculations were performed to test this. The same simulations were then made using the force-field. Figure 4 shows the torsion between a terminal hydrogen (figure 3(a)), terminal oxygen (figure 3(b)), terminal titanium (figure 3(c)) and a surface oxygen (figure 3(c)) for two adjacent hydrogens as a function of simulation time. Zero on the *y*-axis is set as the torsion at the start of the simulation, given a hydrogen-bonded pattern as shown in figure 1(a). It can be seen that there is mostly an anti-correlation between adjacent hydrogens in both PDFT and classical simulations. This shows that the hydrogens will move away from each other in a periodic manner. It also shows agreement between the force-field and DFT.

### 3.3 PDFT calculations of water on the bare $TiO_2$ (110) surface

Water was optimized on the bare surface using PDFT. An optimization using the force-field yielded a different structure as seen in figure 5. As a result, an extra VDW term with a $\sigma_i$ of 3.7 Å and $\varepsilon_i$ of $-0.032$ kcal mol$^{-1}$, fitted from the Buckingham potential interaction of Predota *et al.* [21] was added between the five-coordinated titanium and the water oxygen (table 1). Figure 5 shows the geometry from the force-field optimization when the term has been added in comparison to when it was not. It shows a much better comparison to the PDFT structure.

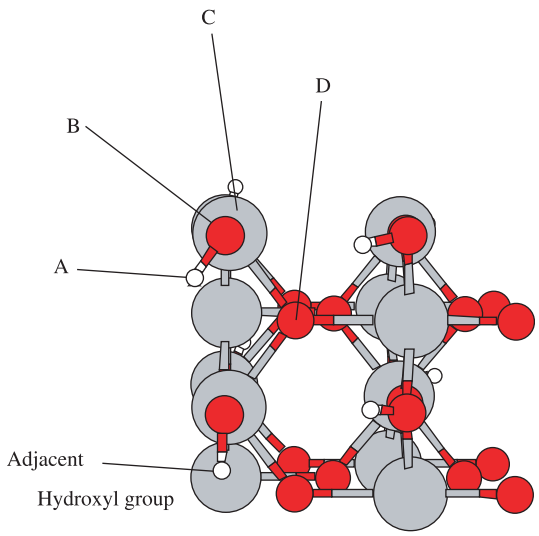


Figure 3. Plan view of the $TiO_2$ (110) surface showing the four atoms which define the torsion (A–D) and adjacent hydroxyl.

The interaction energy was calculated using the following equation

$$E_{\text{int}} = E_{\text{H}_2\text{O+surf}} - E_{\text{H}_2\text{O}} - E_{\text{surf}} \quad (1)$$

where the interaction energy is the energy difference between the energy of the water on the surface and the equivalent of the water molecule at infinite separation.

### 3.4 PDFT calculations of water on the fully hydroxylated surface

Optimizations using three different adsorption geometries were done using PDFT and interaction energies were calculated. The interaction energies were then calculated using the force-field allowing hydroxyl hydrogens to move. In table 4, it can be seen that despite the energies being different, the relative ordering is correct. Figure 6 shows the structures after the optimizations. For the first minimum (figure 6(a)), calculations show both terminal oxygen donors to the water hydrogens and water oxygen donors to bridging hydrogens. The second set of minima (figure 6(b)) are both terminal and bridging oxygen donors to water hydrogens. However, it should be noted that terminal bridging hydrogen also interacts with the water oxygen when optimized using the force-field, causing a flattening of the water on the surface. The third set (figure 6(c)) are both terminal oxygen donors to water hydrogens. In all three cases, the hydrogen-bonded pattern of hydroxyls on the surface has stayed the same.

## 4. MD Simulations of the $TiO_2$–water interface

Axial density profiles of water hydrogen and oxygen were calculated for all kinds of surface considered here. These give the average density over all configurations as a function of distance from the surface plane. The baseline for the surface was taken as the *z*-position of the five-coordinated titanium in non-hydroxylated surfaces and the saturated terminal titanium in hydroxylated surfaces. The results are summarised in figures 7 and 8 and table 5. The oxygen profile for the neutral non-hydroxylated surface shows a peak at 1.4 Å which corresponds to the bridging oxygen, a peak at 2.6 Å which is the first layer oxygen and a peak at 3.9 Å for the second water layer. The defined peaks show that the water is very ordered on this surface and the ordering propagates far from the surface. The negative non-hydroxylated surfaces show similar features with the addition of an extra peak at 2 Å which corresponds to the extra terminal oxygens with the density being greater for the 25% surface than 12.5% surface. The hydrogen profile shows a peak at 3 Å corresponding to the first layer of adsorbed water and peaks at 4.4 and 5.5 Å which are ascribed to the two hydrogens of the second layer water. The negative non-hydroxylated surfaces give similar features plus the addition of an extra terminal hydroxyl peak at 2.2 Å.

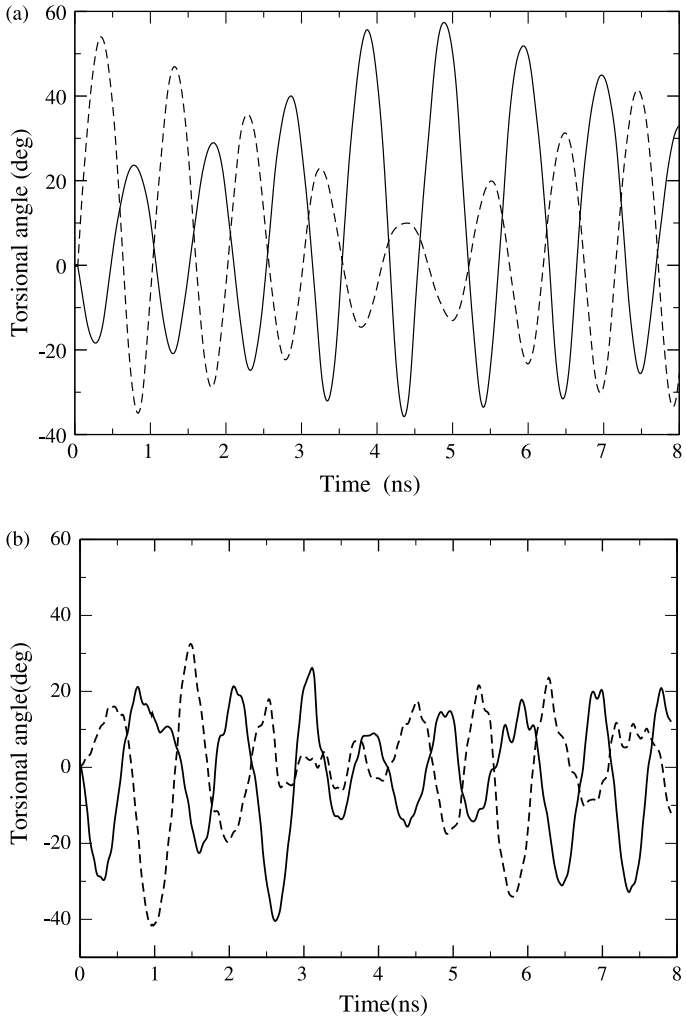


Figure 4. Torsion for two adjacent terminal hydrogens (solid and dashed lines) as a function of simulation time using CPMD (a) and force-field simulations (b).



The oxygen profile for the hydroxylated surface gives two peaks at 1.4 and 1.9 Å which correspond to the bridging and terminal oxygens, respectively. The peak at 3.5 Å corresponds to the next layer of water. The negative surfaces give similar density profiles. The hydrogen profile of the neutral hydroxylated surface shows the bridging and terminal hydrogens at 1.6 and 2.4 Å. The peak at 3.4 Å corresponds to the second layer water. The neutral hydroxylated surfaces show similar features.

In conjunction with the axial density profiles, the angular distribution of water was measured. The average angle between the water dipole and the surface normal

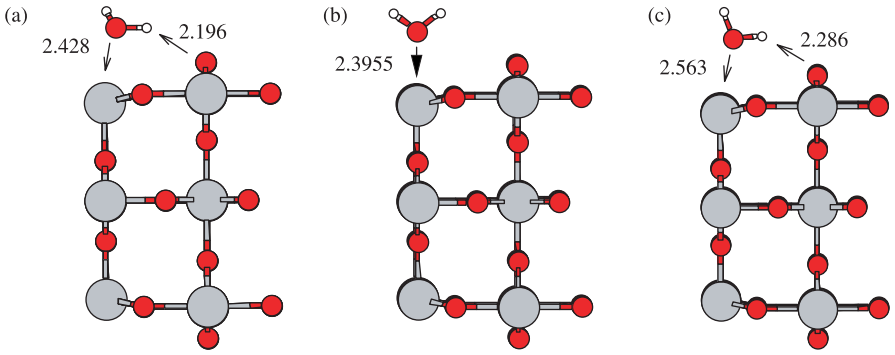


Figure 5. Geometries of water adsorbed on the non-hydroxylated surface of $TiO_2$ rutile (110) after optimization using PDFT (a) and the force field with (c) and without (b) the extra VDW pairwise interaction. Distances are in Å.

Table 4. PDFT and force field interaction energies before and after force-field optimization for three fully hydroxylated five-layer $TiO_2$ surfaces.

| *Surface* | *PDFT (kcal mol$^{-1}$)* | *Force field (kcal mol$^{-1}$)* | *After optimization (kcal mol$^{-1}$)* |
|---|---|---|---|
| Min1 | − 14.10 | − 17.61 | − 19.24 |
| Min2 | − 3.33 | − 6.601 | − 10.85 |
| Min3 | − 4.95 | − 8.12 | − 12.81 |

Min1–Min3 are shown in figure 6.

is plotted as a function of distance from the surface. Figure 9(a) shows that for the neutral non-hydroxylated surface the first layer of waters point their dipoles away from the surface and hence the oxygen points toward the titanium as in figure 5. This peak at 2.2 Å corresponds to the first peak in the axial density profile. The second layer water molecules face the opposite direction with the hydrogens facing towards the surface and this is indicated by the depletion at around 3.9 Å. There is ordering out to 8 Å with depletions followed by peaks, getting less ordered with increasing distance.

There is less ordering for the neutral hydroxylated surface with second layer hydrogens facing towards the bulk water as opposed to the surface in the non-hydroxylated case and to a lesser extent (peak heights of 0.1 compared to 1.0). In the next layer of waters, the hydrogens face towards the the surface on average.

The negative non-hydroxylated surfaces follow the same pattern as the neutral hydroxylated surface except they always have a greater tendency for the hydrogen to face the surface, i.e. the distribution is shifted downwards.

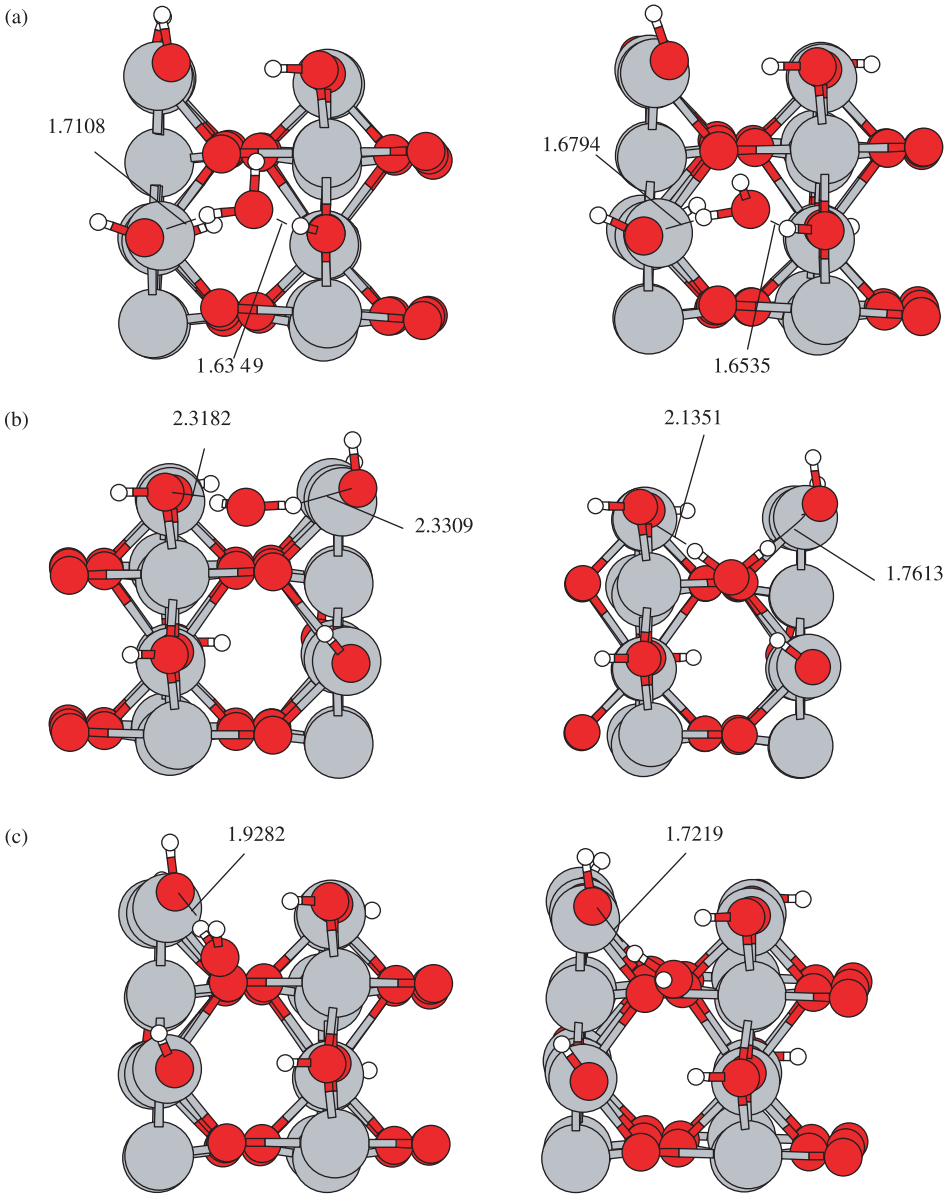


Figure 6. Water on the hydroxylated surface of rutile $TiO_2$ (110) after optimization using PDFT (left) and the force field with (right) for min1 (a), min2 (b) and min3 (c). Distances are in Å.

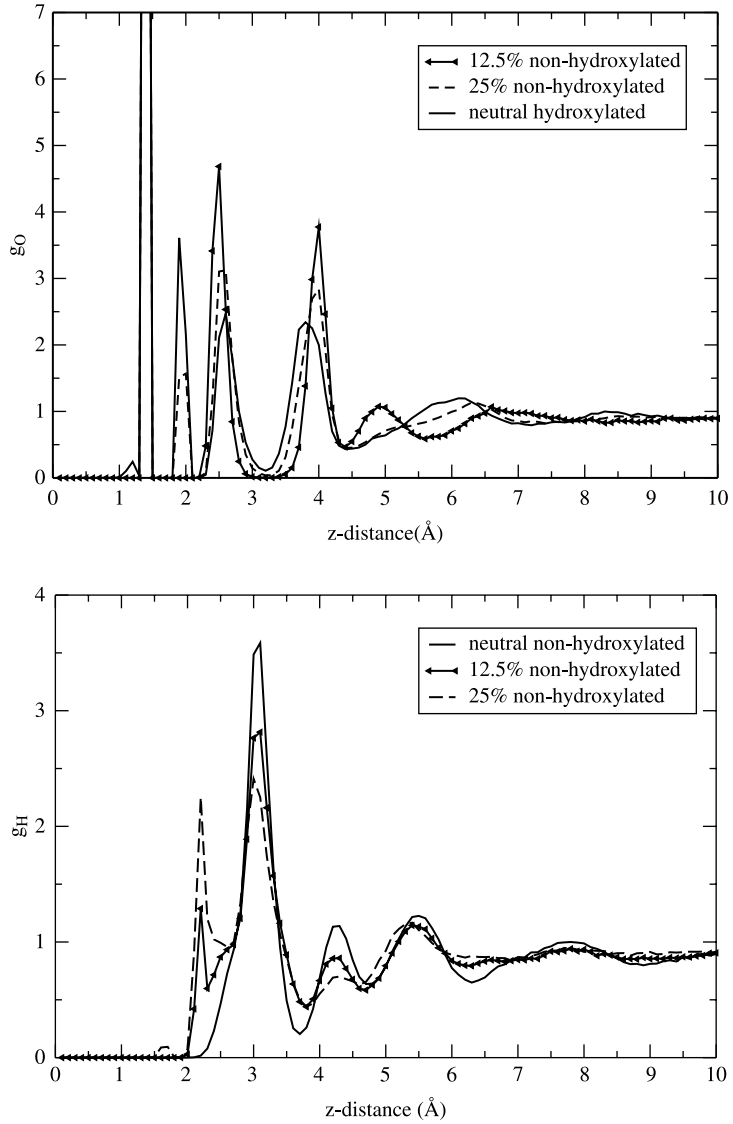




Figure 7. Axial density profile (as a function of $z$-distance) of oxygen (top) and hydrogen (bottom) for the neutral non-hydroxylated and negative non-hydroxylated surfaces.

This is because the positively charged hydrogens have an affinity for the negatively charged surface.

The negative hydroxylated surfaces show a different angular distribution to the neutral hydroxylated surface. Firstly, the cosine remains below 0 until the distance from the surface becomes large. On closer inspection, it can be seen that the ordering is similar to the non-hydroxylated surface, with peaks and depletions occurring at approximately the same distances.

This ordering is not so profound in the 12.5% surface as in the 25% surface. This shows that removal of some of the terminal hydroxyls will cause orientational preferences more like the non-hydroxylated surface than for the hydroxylated surface. The cosine distribution always stays below zero because of the affinity of hydrogens to the negative surface as in the negative non-hydroxylated surfaces.

There is good agreement between the axial density and angular distributions profiles and those of Predota *et al.* [21] (tables 5 and 6) considering the structural model is slightly different. This gives evidence that TIP3P water can match SPC/E water for modelling the rutile–water interface, especially given that the TIP3P model we use here explicitly models VDW effects for the hydrogens on water. There is also agreement between the simulations and X-ray experiments [37] (table 5). Peaks in these experiments show oxygen average distances from the surface. Crystal truncation rod experiments by Zhang *et al.* [37] show a peak at 1.2 Å corresponding to the bridging oxygen which is 1.4 Å in this study. A peak at 2.12 Å corresponds to the terminal oxygen which is at 1.9 Å for the fully hydroxylated surface or first layer water oxygen which is at 2.6 Å for the non-hydroxylated surface. There are peaks from 3.5 to 4.0 Å which correspond to the third

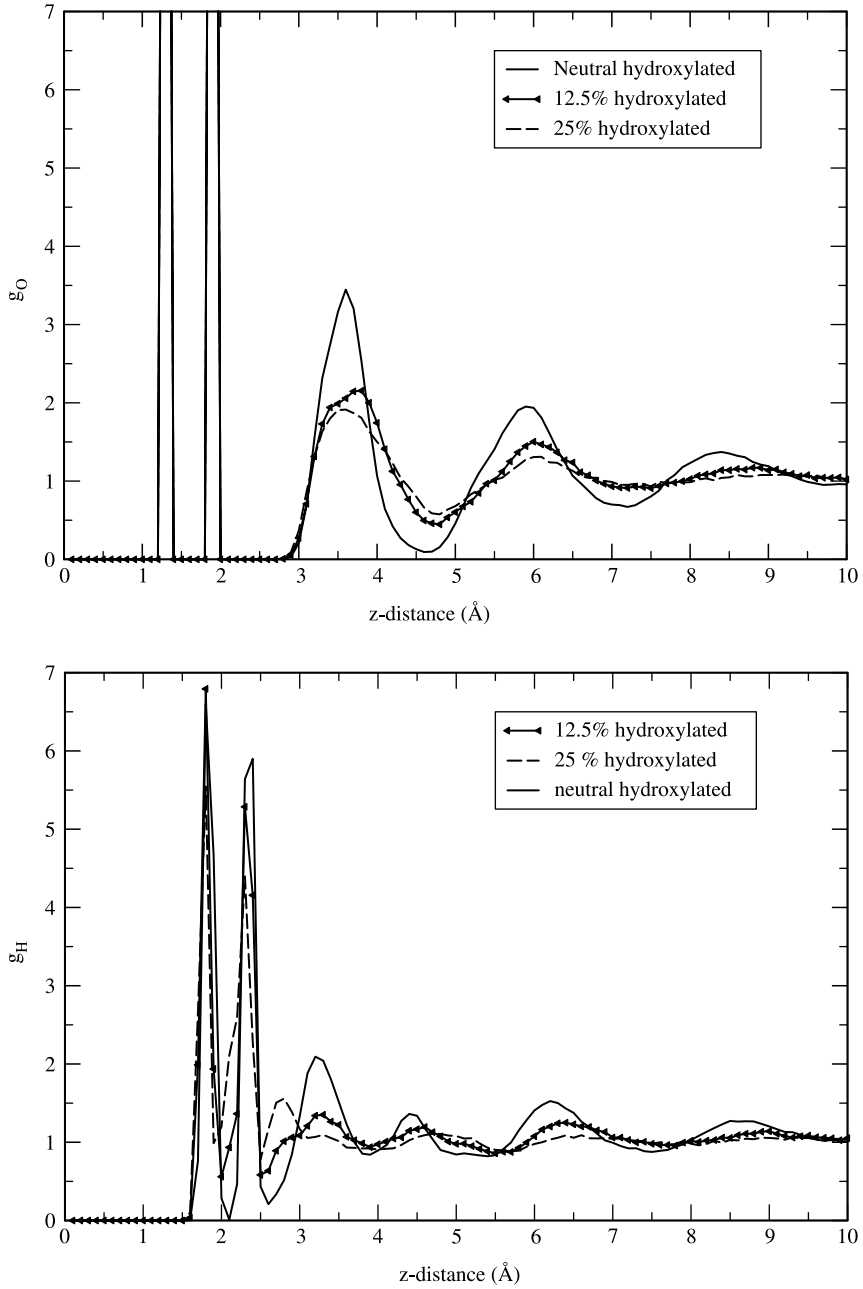


Figure 8. Axial density profile (as a function of $z$-distance) of oxygen (top) and hydrogen (bottom) for the neutral hydroxylated and negative hydroxylated surfaces.

Table 5. $z$-distances of oxygen from terminal titanium for this work, Predota *et al.* [21] and X-ray experiments [37] (values for X-ray experiments are shown in hydroxylated rows for convenience only).

| *Oxygen type* | *z-distance O (Å)* | *Predota O (Å)* | *Experiment* |
|---|---|---|---|
| Bridging bare | 1.3 | 1.3 | – |
| Bridging, hydroxylated | 1.4 | 1.4 | 1.2 |
| Terminal hydroxylated | 1.9 | 2.00 | 2.1 |
| First layer non-hydroxylated | 2.5 | 2.5 | – |
| Second layer non-hydroxylated | 4.0 | 3.8 | – |
| Second layer hydroxylated | 3.6 | 3.7 | 3.5 |

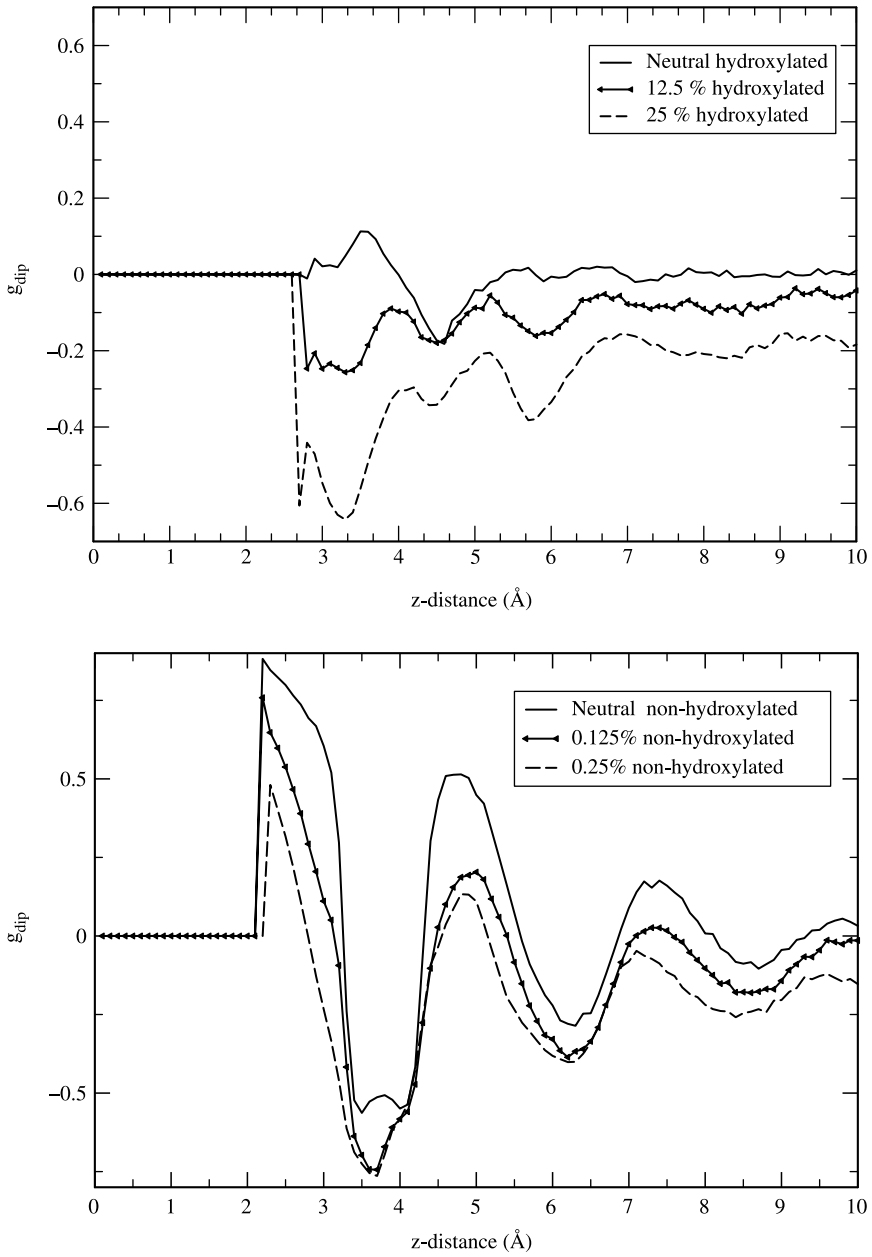


Figure 9. Angular distribution of water (as a function of $z$-distance) for the non-hydroxylated surfaces (top) and hydroxylated surface (bottom).



water layer which is 4.0 Å for the non-hydroxylated surface and 3.6 Å for the hydroxylated surface.

## 5. Conclusion

A force-field which describes the interaction between the rutile $TiO_2$ (110) surface and TIP3P water was tested for three different water–surface adsorption geometries and minor modifications have been made to the existing force-field of Predota *et al.* [21]. The optimization of water on the non-hydroxylated surface using the force-field showed good agreement of the final structure with the PDFT optimized structure, especially for the bond distances. Three structures were examined for water adsorbed on the hydroxylated surface. They showed the same binding geometries and ordering of interaction energies for the force-field and PDFT optimizations. The torsional profile for terminal hydrogens showed good agreement between force-field and PDFT calculations also. The force-field

Table 6. $z$-distances of hydrogen from terminal titanium for this work and that Predota *et al.* [21].

| *Hydrogen type* | *z-distance H (Å)* | *Predota H (Å)* |
|---|---|---|
| Bridging hyd | 1.8 | 2.1 |
| Terminal hyd | 2.4 | 2.5 |
| First layer non-hydroxylated | 3.0 | 2.9 |
| Second layer non-hydroxylated | 4.4, 5.5 | 4.2, 5.3 |
| Second layer hydroxylated | 3.2 | 3.2 |

parameters were altered so that optimization of the hydroxylated surface yielded a structure similar to that of the structure optimized with PDFT.

Simulations of water on six different surfaces were performed. Neutral non-hydroxylated, neutral hydroxylated, negative non-hydroxylated and negative hydroxylated (with the negative surfaces each having two different surfaces of differing charge density) were simulated. The structure of water at the surfaces was analyzed by examining the axial density and angular distribution of water. The axial density profiles showed that both non-hydroxylated and hydroxylated surfaces give similar results. They yield the first layer oxygens at 1.9–2.5 Å and second layer oxygens 3.6–4.0 Å. The results are also in agreement with X-ray truncation rod studies [37] and simulations using SPC/E water [21]. The angular distribution shows that the second layer waters for the neutral hydroxylated surfaces are orientated differently than second layer water on non-hydroxylated surfaces. This seems to alter when terminal hydroxyls are removed as in the negative hydroxylated surfaces. The results are in agreement with simulations using SPC/E water [21]. This work shows that TIP3P water can be used for modelling aqueous $TiO_2$ interfaces and it is therefore viable for use in future studies of biological systems with $TiO_2$ in water.



## Acknowledgements

The authors gratefully acknowledge the computer facilities of the Centre for Scientific Computing, University of Warwick. We thank the University of Warwick for the WPRF funding for A.S. Part of the funding also comes from the EPSRC Material Consortium "Modelling the Biological Interface with Materials", GR/S80127/01.

## References

[1] W. Stumm. *Chemistry of the Solid–Water Interface*, John Wiley and Sons, (1992).
[2] E. Topoglidis, A.E.G. Cass, B. O'Regan, J.R. Durrant. Immobilisation and bioelectrochemistry of proteins on nanoporous $TiO_2$ and ZnO films. *J. Electroanal. Chem.*, **517**, 20 (2001).
[3] E. Topoglidis, C.J. Campbell, A.E.G. Cass, J.R. Durrant. Photoelectrochemical study of Zn cytochrome-c immobilised on a nanoporous metal oxide electrode. *Langmuir*, **17**, 7899 (2001).
[4] E. Topoglidis, T. Lutz, R.L. Willis, C.J. Barnet, A.E.G. Cass, J.R. Durrant. Protein adsorption on nanoporous $TiO_2$ films: a novel approach to studying photoinduced protein/electrode. *Faraday Discuss.*, **116**, 35 (2000).
[5] S.R. Whaley, D.S. English, E.L. Hu, P.F. Barbara, A.M. Belcher. Selection of peptides with semiconductor binding specificity for directed nanocrystal assembly. *Nature*, **405**, 665 (2000).
[6] U. Diebold. The surface science of titanium dioxide. *Surf. Sci. Rep.*, **48**, 53 (2003).
[7] U. Diebold. Structure and properties of $TiO_2$ surfaces: a brief review. *Appl. Phys. A*, **76**, 681 (2003).
[8] R. Schaub, P. Thostrup, N. Lopez, E. Logsgaard, I. Stensgaard, J.K. Norskov, F. Besenbache. Oxygen vacancies as active sites for water dissociation on rutile $TiO_2$(110). *Phys. Rev. Lett.*, **87**, 266104 (2001).
[9] M. Henderson. *Surf. Sci.*, **355** (1996).
[10] P.J.D. Lindan, J. Muscat, S. Bates, N.M. Harrison, M. Gillan. *Faraday Discuss. Chem. Soc.*, **06**, 135 (1997).
[11] P.J.D. Lindan, N.M. Harrison, J.M. Holender, M.J. Gillan. *Chem. Phys. Lett.*, **261**, 246 (1996).
[12] P.J.D. Lindan, N.M. Harrison, M.J. Gillan. Mixed dissociative and molecular adsorption of water on the rutile (110) Surface. *Phys. Rev. Lett.*, **80**, 762 (1998).
[13] A. Fahmi, C. Minot. A theoretical investigation of water adsorption on titanium dioxide surfaces. *Surf. Sci.*, **304**, 343 (1994).
[14] T. Bredow, K. Jug. Theoretical investigation of water adsorption at rutile and anatase surfaces. *Surf. Sci.*, **327**, 398 (1995).
[15] C. Zhang, P.J.D. Lindan. Multilayer water adsorption on rutile $TiO_2$(110): A first-principles study. *J. Chem. Phys.*, **118**, 4620 (2003).
[16] A.S. Barnard, P. Zapol, L.A. Curtiss. Modelling the morphology and phase stability of $TiO_2$ nanocrystals in water. *Surf. Sci.*, **582**, 173 (2005).
[17] M. Matsui, M. Akaogi. Molecular dynamics simulation of the structural and physical properties of the four polymorphs of $TiO_2$. *Mol. Simul.*, **6**, 239 (1991).
[18] A.V. Bandura, J.D. Kubicki. Derivation of force field parameters for $TiO_2$-$H_2O$ systems from *ab Initio* calculations. *J. Phys. Chem. B*, **107**, 11072 (2003).
[19] M. Predota, Z. Zhang, P. Fenter, D.J. Wesolowski, P.T. Cummings. Electric double layer at the rutile (110) surface. 2. Adsorption of ions from molecular dynamics and X-ray experiments. *J. Phys. Chem. B*, **108**, 12061 (2004).
[20] A.V. Bandura, D.G. Sykes, V. Shapovalov, T.N. Troung, J.D. Kubicki, R.A. Evarestov. Adsorption of water on the $TiO_2$ (rutile) (110) surface: A comparison of periodic and embedded cluster calculations. *J. Phys. Chem. B*, **108**, 7844 (2004).
[21] M. Predota, A.V. Bandura, P.T. Cummings, J.D. Kubicki, D.J. Wesolowski, A.A. Chialvo, M.L. Machesky. Electric double layer at the rutile (110) surface. 1. Structure of surfaces and interfacial water from molecular dynamics by use of *ab initio* potentials. *J. Phys. Chem. B*, **108**, 12049 (2004).
[22] V. Carravetta, S. Monti. Peptide-$TiO_2$ surface interaction in solution by *ab initio* and molecular dynamics simulations. *J. Phys. Chem. B*, 6160 (2006).
[23] S.J. Weiner, P.A. Kollman, D.A. Case, U.C. Singh, C. Ghio, G. Alagona, S. Profeta, P. Weiner. A new force field for molecular mechanical simulation of nucleic acids and proteins. *J. Am. Chem. Soc.*, **106**, 765 (1984).
[24] S.J. Weiner, P.A. Kollman, D.T. Nguyen, D.A. Case. An all atom force field for simulations of proteins and nucleic acids. *J. Comp. Chem.*, **7**, 230 (1986).
[25] W.L. Jorgenson. Quantum and statistical mechanical studies of liquids. 10. Transferable intermolecular potential functions for water, alcohols, and ethers. Application to liquid water. *J. Am. Chem. Soc.*, **103**, 335 (1981).
[26] P. Mark, L. Nilsson. Structure and dynamics of the TIP3P, SPC, and SPC/E water models at 298 K. *J. Phys. Chem. A*, **105**, 9954, (2001).
[27] J.A.D. MacKerell, D. Bashford, M. Bellott, R.L. Dunbrack Jr., J.D. Evanseck, M.J. Field, S. Fischer, J. Gao, H. Guo, S. Ha, D. Joseph-McCarthy, L. Kuchnir, K. Kuczera, F.T.K. Laux, C. Mattos, S. Michnick, T. Ngo, D.T. Nguyen, B. Prodhom, I.W.E. Reiher, B. Roux, M. Schlenkrich, J.C. Smith, R. Stote, J. Straub, M. Watanabe, J. Wiorkiewicz-Kuczera, D. Yin, M. Karplus. All-atom empirical potential for molecular modelling and dynamics studies of proteins. *J. Phys. Chem. B*, **102**, 3586 (1998).
[28] K.I. Sano, K. Shiba. A hexapeptide motif that electrostatically binds to the surface of titanium. *J. Am. Chem. Soc.*, 14234 (2003).
[29] J.W. Ponder, S. Rubenstein, C. Kundrot, S. Hustonand, M. Dudek, Y. Kong, R. Hart, M. Hodsdon, R. Pappu, W. Mooij, G. Loeffler, M. Vorobieva, N. Sokolova, P. Bagossi, P. Ren, A. Carlsson, A. Kutepov, A. Grossfield, M. Schnieders. *TINKER*, Version 4.2, (2004).
[30] M.D. Segall, P.J.D. Lindan, M.J. Probert, C.J. Pickard, P.J. Hasnip, S.J. Clark, M.C. Payne. First-principles simulation: ideas, illustrations and the CASTEP code. *J. Phys. Cond. Matt.*, **14**, 2717 (2002).
[31] M. Ramamoorthy, D. Vanderbilt. First-principles calculations of the energetics of stoichiometric $TiO_2$ surfaces. *Phys. Rev. B*, **49**, 16721 (1994).

[32] B. Hammer, L.B. Hansen, L.K. Norskov. Improved adsorption energetics within density-functional theory using revised Perdew–Burke–Ernzerhof functionals. *Phys. Rev. B*, **B59**, 7413 (1999).

[33] E. Spohr. Molecular dynamics simulation studies of the density profiles of water between (9-3) Lennard–Jones walls. *J. Chem. Phys*. **106**, 388 (1997).

[34] S.C. Abrahams, J.L. Bernstein. Rutile : Normal probability plot analysis and accurate measurement of crystal structure. *J. Chem. Phys.*, **55**, 3206 (1971).

[35] J.K. Burdett, T. Hughbanks, G.J. Miller, J.W. Richardson, J.V. Smith. Structural-electronic relationships in inorganic solids: Powder neutron diffraction studies of the rutile and anatase polymorphs of titanium dioxide at 15 and 295 K. *J. Am. Chem. Soc.*, **109**, 3639 (1987).

[36] L. Verlet. Computer "experiments" on classical fluids. I. Thermodynamical properties of Lennard–Jones molecules. *Phys. Rev.*, **159**, 98 (1967).

[37] Z. Zhang, P. Fenter, L. Cheng, N.C. Sturchio, M.J. Bedzyk, M. Predota, A. Bandura, J.D. Kubicki, P.T.C.S.N. Lvov, A.A. Chialvo, M.K. Ridley, P. Banazeth, L.A.D.A. Palmer, M.L. Machesky, D.J. Wesolowski. Ion Adsorption at the rutile-water interface: Linking molecular and macroscopic properties. *Langmuir*, **20**, 4954 (2004).